Title

Intrinsic apoptosis is evolutionarily divergent among metazoans

Authors

Gabriel Krasovec [1,2,3*], Éric Quéinnec [1**], Jean-Philippe Chambon [2,4**]

[*] Authors for correspondence:

GK, gabriel.krasovec@nuigalway.ie; gabrielkrasovec@hotmail.fr

[**] These authors contributed equally to this work.

Affiliations

[1]ISYEB, Institut de Systématique, Evolution et Biodiversité, Sorbonne Université, CNRS, MNHN, F-75252 Paris Cedex 05, France.

[2]Sorbonne Université, CNRS, Institut de Biologie Paris Seine, IBPS, Evolution Paris Seine, F-75252 Paris Cedex 05, France.

[3]Centre for Chromosome Biology, School of Natural Sciences, National University of Ireland Galway, Galway, Ireland.

[4]Centre de Recherche de Biologie Cellulaire de Montpellier (CRBM), Montpellier Univ., CNRS, 34000 Montpellier, France.

Abstract

Apoptosis is regulated cell death that depends on caspases. Upstream of each apoptotic signalling pathway is involved a specific initiator caspase. Characterized in nematode, fly and mammals, intrinsic apoptosis is considered to be ancestral and conserved among animals, and depends on shared initiators; caspase-9*,* Apaf-1 and Bcl-2. However, the biochemical role of mitochondria, the pivotal function of cytochrome c and the modality of caspase activation remain highly heterogeneous and hide profound molecular divergences among apoptotic pathways in animals. Uncovering the phylogenetic history of apoptotic actors, especially caspases, is crucial to shed light on intrinsic apoptosis evolution. Here, we demonstrate by phylogenetic analysis, that caspase-9, the fundamental key of intrinsic apoptosis, is deuterostome-specific, while caspase-2 is ancestral to bilaterians. Our analysis of Bcl-2 and Apaf-1 confirm heterogeneity in functional organisation of apoptotic pathways in animals. Our results support convergent emergence of distinct intrinsic apoptotic pathways during metazoan evolution.

49 **INTRODUCTION**

50 Apoptosis, regulated cell death defined by a set of morphological features and
51 dependent on caspases, occurs during metazoan development, tissue homeostasis, and
52 regeneration[1–3]. Pioneering works in *Caenorhabditis elegans* established a molecular network
53 of apoptosis decision, execution, engulfment-degradation, and more fundamentally the first
54 description of intrinsic apoptosis, previously known as the mitochondrial apoptotic pathway[4–
55 6]. Next, investigation of apoptotic cascade key components from *Drosophila melanogaster* and
56 mammals imposed the paradigm that the intrinsic apoptotic "molecular program" is
57 conserved throughout animal evolution[4,5,7–9]. Intrinsic apoptosis depends on the key initiator
58 caspase-9 (named Ced-3 and Dronc in *Caenorhabditis* and *Drosophila*, respectively), the
59 activator Apaf-1 (named Ced-4 and Dark in *Caenorhabditis* and *Drosophila*, respectively) and
60 the Bcl-2 multigenic family[4,8]. However, recent research has revealed evolutionary
61 divergences between these models, with major functional implications[10,11]. Importantly and
62 independently of functional approaches, the phylogenetic history of the signal transduction
63 actors, mostly the caspase family, is the Rosetta Stone to shed light on intrinsic apoptosis
64 evolution. Here, we investigate the evolutionary history of the major actors of intrinsic
65 apoptosis. We conducted phylogenetic analyses of initiator CARD-caspases, Bcl-2 multigenic
66 family, and Apaf-1 proteins from major animal phyla and describe their evolutionary patterns.
67 It is apparent that despite common functional similarities, these actors, especially initiator
68 caspases, have distinct evolutionary histories. Consequently, we consider the structural and
69 functional organisation of intrinsic apoptotic components to be the result of evolutionary
70 convergence among animals. Thus, the three animal models (nematode, fly, mouse) which
71 were used to establish a unified concept of intrinsic apoptosis, in addition to present
72 functional divergences, are also markedly by distinct origin of their molecular apoptotic actors.

RESULTS AND DISCUSSION

Initiator caspases of intrinsic apoptotic pathways are not homologous genes

Initiation and execution of apoptotic signalling pathways are fundamentally linked to the complex diversification of caspases which are widely distributed among all metazoan phyla[12–15].

Caspases are a class of proteases composed of three protein domains; the pro-domain, the small P10, and the large P20[16,17]. Initiator caspases, specific to each apoptotic pathway, have a Caspase Recruiting Domain (CARD) pro-domain or two Death Effector Domains (DED) pro-domains. Intrinsic and extrinsic apoptosis are distinct and involve specific initiators which are caspase-9 (CARD pro-domain) or caspase-8 or -10 (DED pro-domains), respectively. Both pathways trigger activation of common executioner caspases, leading to apoptosis execution[4,18].

Due to the pivotal role of caspase-9 in initiating intrinsic apoptosis, our main analyses focused on caspases having a CARD pro-domain (CARD-caspases). We confirmed their distribution in most animal phyla and reconstructed their phylogenetic relationships (Figure 1, Table S1). Regardless of the phylogenetic methodology used for the analysis, two strongly supported (PP> 0.99) monophyletic groups were identified: caspase-9 and caspase-2 (Figure 1, Figure S1). A third and more heterogeneous group named here [Inflammatory Caspases + Caspase-Y] is monophyletic in Bayesian analysis, the method which produced the most likely topology (Table S2), and splits into two groups in maximum likelihood estimation (Figure 1, Figure S1). Although relationships among bilaterian clades differ depending on the methodology employed, monophyly of caspase-9 and caspase-2 families remains robust. They group together with Inflammatory Caspases and Caspase-Y in a clade strictly diversified within bilaterian animals (PP = 0.87; BS>90). The sequences of non-bilaterians [Cnidaria + Ctenophora

97 + Placozoa] form a divergent paraphyletic group named here Caspase-X (Figure 1). Switching
98 between metazoan putative "basal" out groups [i.e. *Amphimedon queenslandica* (Porifera) or
99 *Pleurobrachia bachei* (Ctenophora)] does not affect caspase topology (Figure S2). All
100 bilaterians sequences, caspase-9, caspase-2 and [Inflammatory Caspases + Caspase-Y] remain
101 monophyletic (Figure S2).

102 Caspase-2 appears to be widely distributed among bilaterians and sequences evolution
103 is congruent with the bilaterian groups [Deuterostomia + Ecdysozoa +
104 Lophotrochozoa/Spiralia] reflecting its ancestral origin. Surprisingly caspase-9 is strictly
105 restricted to deuterostome animals. This distribution can be interpreted either as the early
106 emergence of caspase-9 in all bilaterians followed by a secondary loss in protostomes, or as a
107 specific derived character of deuterostomes. The diversity of the genomes explored, and their
108 depth of sequencing unambiguously confirms this result. More specifically, the robustness of
109 the deuterostome caspase-9 clade was explored (Figure S3), and its specific diversification
110 among [Vertebrata + Cephalochordata + Echinodermata + Hemichordata] was confirmed.
111 However, the relative position of the cephalochordate *Branchiostoma belcheri* 9A paralogous
112 gene remains unstable. Consistent with previous studies on the ascidian *Ciona intestinalis*[19],
113 the five representatives of ascidian genomes studied are devoid of any caspase-9, likely due
114 to a unique secondary loss in urochordates, the sister-group of vertebrates[20].

115 Unexpectedly, *Drosophila* Dronc and *Caenorhabditis* Ced-3 are distinctly identified as
116 orthologous (i.e. coming from speciation) to caspase-2 of vertebrates, and not to caspase-9,
117 as was previously reported and largely accepted[21–28]. All Dronc/Ced3 proteins of insects,
118 horseshoe crab (Xiphosura), and nematodes form a strongly supported monophyletic clade
119 (PP = 1) revealing single gene conservation without duplication (except horseshoe crab). Thus,
120 the caspase-2 clade of ecdysozoans is the sister group of caspase-2 clade of [Lophotrochozoa

121 + Deuterostomia]. The absence of identifiable caspase-2 in echinoderms and hemichordates
122 can probably be interpreted as a specific later loss (i.e. Ambulacraria).
123 Conversely, the clade [Caspase-Y + Inflammatory Caspase] appears to be restricted to
124 [Vertebrata and Lophotrochozoa].
125 Taken globally, our analysis shows that the traditionally considered conserved initiator
126 caspases of intrinsic apoptosis are not orthologous, but divergent genes putatively issued from
127 ancestral duplication among bilaterians.
128
129 **The caspase activation regulator apoptosome is highly divergent in metazoans**
130 In intrinsic apoptosis, initiator caspase activation depends on their recruitment by a
131 pivotal, and considered shared component, the apoptosome platform[4,10]. Apoptosome
132 formation results on critical protein interaction between *Caenorhabditis* Ced-4, *Drosophila*
133 Dark, and human Apaf-1 with their respective initiator caspases Ced-3, Dronc, and procaspase-
134 9, respectively[10]. CARD and other domains (NOD, arm) are highly conserved in Apaf-1, Dark
135 and Ced-4 proteins[29–31]. However, excepted the majority of nematode species[11], Apaf-1
136 possesses WD40 repeats at its C-terminus which bind to cytochrome c. This binding is required
137 in mammals for Apaf-1 oligomerisation and apoptosome formation[31,32], while Ced-4 and Dark
138 do not require cytochrome c for their general assembly into an apoptosome[10,33]. Taken with
139 major structural and regulating assembly differences between the octameric Dark, tetrameric
140 Ced-4 and heptameric Apaf-1 apoptosomes, it reveals evolutionary divergence between
141 animal apoptosomes formation and procaspases activation mechanisms, probably
142 differentially modulating the cell death execution pathway[34].
143 We conducted exhaustive analysis by reciprocal BLAST and phylogenetic analyses of
144 Apaf-1 homologs and confirmed their conservation in the majority of metazoan phyla (Figure

145 S4, Table S3)[29,30]. Our topology presents two main clades that are common between Bayesian
146 inference method and maximum likelihood estimation, both of which are inconsistent with
147 species phylogeny. One of them grouped ecdysozoan sequences including Ced-4 and Dark,
148 while the other one contains deuterostomian and non-bilaterian sequences. Unexpectedly,
149 deuterostomians are not monophyletic but split into two groups, suggesting classic long
150 branch attraction artifact and a very fast sequence evolution. Remarkably, Apaf-1 was absent
151 from all available urochordate and mollusc genomes, in accordance with previous work[19,30,35–
152 38], and from *Capitella teleta* (Annelida). Even if differences in the quality of the genomes might
153 account for some of the putative losses, these results suggest independent losses in
154 urochordates and lophotrochozoans or, a less parsimonious hypothesis, complex and
155 independent modular protein evolution from the common ancestor of metazoans (Figure 2).
156 In non-bilaterians, the Apaf-1 gene family has not been found in the *Pleurobrachia pileus*
157 genome (Ctenophora), but seems present in other early diverging metazoan phyla [Porifera,
158 Cnidaria and Placozoa] ([30,39,40], our data).

159 Importantly, a previous analysis from several genomes (cnidarian, nematode, fly,
160 amphioxus, sea urchin, human) clearly identified three well-defined independent clades of
161 genes among metazoans, highlighting that Ced-4, Dark and Apaf-1 are not homologous genes
162 between ecdysozoans and vertebrates[30].

163 Despite its fundamental role in the apoptotic cell death pathways and also in non-
164 apoptotic functions[41–43], diverse metazoan phyla have independently experienced adapter
165 protein Apaf-1 losses. Consequently, we may hypothesise a relaxation of functional constrains
166 on molecular Apaf-1-like molecule oligomerisation processes in some phyla, such as molluscs.
167 However, Apaf-1 is under strong purifying selection in the phyla that have not lost it as

168 illustrated by a dN/dS close to 0 (M0 ωθ = 0.07), suggesting a crucial role for this caspase
169 activator.

170 These elements argue in favour of distinct evolutionary trajectory between species,
171 and the convergence of the modality of apoptosome formation, which could explain
172 functional analyses showing that its formation and the subsequent caspase activation differs
173 among taxa[11].

174

175 **The regulation of apoptosis by the Bcl-2 family is convergent among metazoans**

176 Intrinsic apoptosis is ultimately regulated by the Bcl-2 proteins, composed of several
177 Bcl-2 homologous (BH) domains[44,45]. In mammals, the balance between pro-survival (four
178 BH1-BH4 domains) and pro-apoptotic proteins (Bax/Bak/Bok and BH3-only) of Bcl-2 controls
179 initiation of intrinsic apoptosis. Conformational changes of the three-dimensional structures
180 and interactions between Bcl-2 actors enables the assembly of pore-like structures controlling
181 MOMP[46].

182 Multiple sequence alignments of metazoan Bcl-2 family proteins (Supplementary
183 Figure 5, Table S4) (but with over-represented chordates reflective of greater availability of
184 vertebrate genomes) confirm the wide distribution and early origin of Bcl-2 in
185 Metazoa[11,29,45,47]. Proteins clustered into five monophyletic groups, consistent with classical
186 functional Bcl-2 classification (i.e. three 'pro-apoptotic' clades: Bok, Bak, Bax and two less
187 supported pro-survival - 'anti-apoptotic' - groups: Bcl-2/W/XL and a more complex Bcl-B/Mcl-
188 1/Bfl-1 clade) (Figure S5). However, relationships among the five well-supported groups were
189 not clearly resolved despite the use of various methodologies and outgroup selections (Figure
190 S5A-B). Consequently, each of the five Bcl-2 clades seems conserved across evolution, and
191 homology relationships between species inside each clade can be identified. However, due to

192 the impossibility of addressing the relationship between these five monophyletic groups (Bok,
193 Bak, Bax, Bcl-2/W/XL, Bcl-B/Mcl-1/Bfl-1), it is not possible to hypothesises their global
194 evolutionary history, determine a potential ancestral group, or build an evolutionary scenario.
195 In addition, some very divergent sequences from molluscs such as *Biomphalaria glabrata* (Bcl-
196 like2, Bcl-like3), from the cnidarian *Hydra vulgaris* (Bcl-like1) or from the urochordate *Ciona*
197 *intestinalis* (Bcl-like1) were not attributed to a particular class.

198 *Caenorhabditis* is deprived of pro-apoptotic Bcl-2 and possesses only the pro-survival
199 Ced-9 (homolog to vertebrates Bcl-2/w/xl), and two BH-3 only proteins (Egl-1 and Ced-13).
200 Conversely, only two pro-apoptotic Bok-like paralogs (Debcl and Buffy) were present in
201 *Drosophila* (Figure 2, Figure S5), but their functions remain unclear[48]. Presence of both anti-
202 and pro-apoptotic Bcl-2 in molluscs underlines the divergent particularities observed within
203 protostomes. Contrarily, similarities in Bcl-2 family composition are observed within some
204 deuterostomes (mammals and echinoderms).

205 Finally, if multiple Bcl-2 genes were acquired early in metazoan evolution, and despite
206 conservation of almost homologous genes, key differences accumulate, making initiation
207 mechanisms in intrinsic apoptotic signalling pathways convergent among animals.

208

209 **Apoptotic mitochondrial pathways are convergent among metazoans**

210 Functional evidence shows that caspase-2 members play a critical role in various cell
211 death processes, but are independently involved in a range of non-apoptotic functions,
212 including cell cycle regulation, DNA repair and tumour suppression[49–52]. This implication of
213 caspase-2 in a myriad of signalling pathways, and its ability to interact with a panel of
214 molecules, demonstrates its functional versatility[49,50,53–56]. As previously reported, our

215 phylogenetic analyses corroborate the wide distribution of caspase-2 in bilaterians and
216 suggest a probable ancestral multifunctionality.

217 The major structural and functional similarities that led to an erroneous interpretation
218 of the phylogenetic position of Ced-3 and Dronc underlies a probable common evolutionary
219 origin of caspase-2 and -9 genes. We hypothesised here that caspase-9 originates from
220 bilaterians-specific duplication of a caspase-like ancestor, followed by a loss of caspase-9 in
221 protostomians (Figure 2). Among deuterostomians the two families of paralogs have been
222 preserved in vertebrates and probably in cephalochordates (Figure 1, 2). Caspase-2 retains
223 multifunctional activity, and in mammals can interact with the PIDDosome platform
224 containing P53, adapter molecule RAIDD, and signalling complex DISC, activating both
225 extrinsic and intrinsic apoptosis, and DNA damage pathways[55,57–59]. Conversely, the caspase-
226 9 gene underwent a functional divergence in connection with its specialisation in allosteric
227 interactions with the apoptosome[18].

228 Due to its pivotal role as a mediator of genomic stability through involvement in cell
229 proliferation, oxidative stress, aging and cell death, the molecular divergence of the caspase-
230 2 gene is highly constrained during evolution, probably because destabilisation of any
231 signalling cascade is sufficient to initiate tumorigenesis. Therefore, purifying selection is likely
232 important during caspase-2 evolution as illustrated by a dN/dS close to 0 (M0 $\omega\theta = 0.07$)[60,61].
233 However, during the radiation of deuterostomes, both presence of caspase-2 and -9 certainly
234 facilitated the loss of one of them (cf. DCC Force's model -Duplication-Degeneration-
235 Complementation model)[62–64]. Despite purifying selection, a caspase-2 duplication occurred
236 in urochordates in addition to the loss of caspase-9 (Figure 1, Supplementary Figure 2).
237 Similarly, caspase-2 has been lost, or strongly diverged, while caspase-9 presents a *de novo*
238 relative expansion in *Strongylocentrotus purpuratus* (Echinodermata) and *Saccoglossus*

239 *kowalevskii* (Hemichordata). These expansions certainly result from a less powerful purifying
240 selection of caspase-9, having a higher dN/dS (M0 ωθ = 0.22) than caspase-2.

241 Due to generalised gene losses in ecdysozoans and in comparison with other
242 bilaterians, *Caenorhabditis* and *Drosophila* apoptotic pathways are generally considered
243 simpler than those of vertebrates[17,65]. However, comparing to mammals, ecdysozoans have
244 pathways organised around different paralogous genes in addition to a smaller number of
245 genes present. The absence of gene orthologous relationships results in a very different
246 structural organisation of platforms but also generates important functional divergences (i.e.
247 mechanisms of regulating assembly, CARD-CARD interactions with procaspases)[10].

248 Consistent with mammalian caspase-2 functions, Ced-3 has both initiator as well as
249 executioner activities[55,66–68]. Involvement of Dronc in various processes such as compensatory
250 cell proliferation, inhibition of cell migration or spermatid differentiation, brings this protein
251 closer to the functionalities of mammalian caspase-2[69,70]. Due to its interaction with Dark
252 (Apaf-1 paralog), the only CARD-caspase in *Drosophila* (Dronc) has been erroneously classified
253 as caspase-9[8,71]. Unlike the organisation of the mammal apoptosome, both *Caenorhabditis*
254 and *Drosophila* present neither MOMP nor the release and necessity of cytochrome c to
255 activate Ced-3 and Dronc via Ced-4 and Dark, respectively[5,65].

256 Like other protostomes, molluscs are devoid of caspase-9 but caspase-2 has been
257 identified in bivalves and was suspected to function in "a caspase-9-like manner"[72]. Hence,
258 caspase-2 is responsible for apoptotic processes in molluscs, but more surprisingly, despite
259 the absence of caspase-9 and Apaf-1 (and thus, of a mammalian-like apoptosome), this
260 peculiar pathway is surprisingly associated with cytochrome c release[35,38,73–76]. The complexity
261 of intrinsic apoptosis in molluscs seems to be important, but divergent from what was

262 observed in ecdysozoans or vertebrates, with a putative expansion of caspases that
263 participate both in immunity, stress responses, and apoptosis (Figure 2)[38,72,77–80].
264 Unexpectedly, mammals present an almost unique case (possibly with the
265 cephalochordates) in which both caspase-2 and caspase-9 are conserved and involved in
266 apoptosis. This putative functional redundancy (i.e. recruitment, autoactivation or
267 transactivation, homodimerisation and subsequent interchain proteolytic cleavage)
268 undoubtedly led to the functional specialisation observed for caspase-9. This possibly results
269 from the specificity of the mammalian mitochondrial pathway and the non-apoptotic function
270 of caspase-9[81–84]. Finally, echinoderms seem to uniquely have an intrinsic apoptosis similar to
271 mammals, with a caspase-9, Bcl-2, Apaf-1, and a MOMP with cytochrome c release (Figure
272 2)[7,85].
273 Although we can envisage a weak parsimonious scenario that showcases a common
274 ancestral apoptotic pathway in deuterostomes (but implying independent secondary losses in
275 hemichordates, cephalocordates and urochordates), the similarities observed between
276 echinoderms and mammals more probably reflect functional convergences based on
277 independent recruitment of apoptotic actors.
278
279 **CONCLUSION**
280 The apoptotic networks of *Caenorhabditis* and *Drosophila* do not exemplify ancestral
281 conditions from which mammalian-grade apoptotic complexity emerged but are on the
282 contrary, and as suggested recently, the result of a derived condition specific to ecdysozoans
283 among animals [29,77,86,87].
284 The core components of intrinsic apoptotic pathways, especially initiator caspases and
285 the apoptosome platform, are not ancestral in metazoans. Our phylogenetic analyses highlight

286 an unexpected evolutionary history: while the bilaterian caspase-2-mediated apoptotic toolkit
287 emerged ancestrally and remains multifunctional, the caspase-9 mediator of the mammalian
288 apoptosome is specific to deuterostomes.

289 The major functional divergences in mitochondrial apoptotic pathways observed in
290 animals[67,88–90] mainly originated in the recruitment of paralogous actors from the same
291 multigenic families. This reflects an adaptive processes specific to each taxon, which led
292 ultimately to convergent evolutionary histories. Interestingly, this richness of the apoptotic
293 genetic repertoire was suggested to be linked to the persistence of stem cells in adults from
294 different phyla[91,92].

295 Finally, mitochondria-mediated apoptosis, like other programmed cell deaths, has
296 likely evolved before and throughout metazoan diversification to shape developmental
297 processes, immune response, or to adapt cellular environment to environmental constraint.

298

299 **MATERIAL AND METHODS**

300 **Sequence dataset construction**

301 Putative metazoan caspases with a CARD pro-domain (CARD-caspases) were identified
302 using tBLASTn and BLASTp searches with human caspases, Ced-3, and Dronc as queries on
303 NCBI, ANISEED (ascidians), EchinoBase (*Strongylocentrotus purpuratus*), and
304 neurobase.rc.ufl.edu (*Pleurobrachia bachei*) databases, and followed by reciprocal BLAST.
305 After identification of CARD-caspases in target species, sequences were added as queries to
306 conduct BLAST searches in close relatives (i.e. identified CARD-caspases of *Crassostrea gigas*
307 were used as queries to search in other molluscs). Genomes and transcriptomes of species'
308 were downloaded when possible, to search a second time. Sequences with an e-value inferior
309 to 1e-10 were retained. All identified sequences were analysed with ScanProsite (ExPaSy)[93]

310 and InterProScan (EMBL-EBI)[94] to verify the presence of specific caspase domains. Another
311 sequence was added to verify its identification proposed as a caspase-2 in the literature:
312 *Crassostrea angulata* casp-2[76]. Caspase family proteins are short (containing the large
313 common P20 and the small P10 domains) with a high number of genes per species which
314 rapidly limits the relevance of the phylogenetic analyses. To reduce artefact branching and
315 unreadable topologies, and to maximize phylogenetic diversity across Metazoa, the dataset
316 was built using CARD-caspase gene repertoires of selected species. A full list of all caspase
317 sequences is provided in Table S1. Taxon and genes were selected to have a wide diversity of
318 major metazoan phyla and to have an equilibrium inside and between each group. We choose
319 representative species for each phylum and took care to don't unreasonably increase the
320 number of sequences by redundant choice. We privileged species where we detected
321 caspases with CARD domains, DED domains, and executioner caspases, suggesting a high
322 quality of sequences allowing identification of all members of the caspase family. For each
323 taxon, all caspases having a CARD pro-domains have been include in the analysis.

324 Identification of metazoan Apaf-1 was made using tBLASTn and BLASTp using human
325 APAF-1, nematode Ced-4, and fly Dark as queries on NCBI, ANISEED (ascidians), and
326 neurobase.rc.ufl.edu (*Pleurobrachia bachei*) databases, and followed by reciprocal BLAST.
327 Potential resulting sequences were analysed with ScanProsite and also InterProScan. A full list
328 of all Apaf-1 sequences is provided in Table S3.

329 Metazoan Bcl-2 were identified by using tBLASTn and BLASTp searches with human
330 Bcl-2 as the query sequence on NCBI, and then again on downloaded genomes and
331 transcriptomes, followed by reciprocal BLAST. All identified sequences were analysed with
332 ScanProsite (ExPaSy) and InterProScan (EMBL-EBI) to verify the presence of BH domains. Due

333 to short sequence length, BH3-only were not taken into account. A full list of all Bcl-2
334 sequences is provided in Table S4.

335 Multiple alignments of protein sequences were generated using the MAFFT software
336 version 7[95] with default parameters and also Clustal Omega[96] to verify the congruence of the
337 different alignments. All sequences were then manually checked in BioEdit 7.2 software[97] to
338 verify the presence of specific domains previously identified. Gblocks version 0.91b[98] was used
339 to remove vacancies and blur sites. Final alignments comprise of 230, 235, 147, and 513 amino
340 acids for metazoan CARD-caspases alignment, deuterostomian CARD-caspases alignment,
341 metazoan Bcl-2 alignment, and Apaf-1 alignment, respectively.

342

343 **Phylogenetic analysis**

344 Phylogenetic analyses were carried out from the amino-acid alignment with
345 Maximum-Likelihood (ML) method in PhyML 3.1[99], a combined ML tree search with 1000
346 bootstrap replicates was produced and then visualised using Seaview[100]. The best amino-acid
347 evolution models to conduct analyses were determined using MEGA11[101] and determined to
348 be WAG for CARD-caspases alignments (CARD, P20, P10), and LG for Bcl-2 and Apaf-1
349 alignments.

350 Bayesian analyses were performed using MrBayes (v3.2.6)[102] under mixed model. For
351 each analysis, one fourth of the topologies were discarded as burn-in values, while the
352 remaining ones were used to calculate posterior probability. The run for metazoan CARD-
353 caspases alignment was carried out for 2,000,000 generations with 15 randomly started
354 simultaneous Markov chains (1 cold chain, 14 heated chains) and sampled every 100
355 generations. The run for deuterostomian CARD-caspases alignment was carried out for
356 500,000 generations with 5 randomly started simultaneous Markov chains (1 cold chain, 4

357 heated chains) and sampled every 100 generations. The run for metazoan Apaf-1 alignment
358 was carried out for 500,000 generations with 5 randomly started simultaneous Markov chains
359 (1 cold chain, 4 heated chains) and sampled every 100 generations. The run for metazoan Bcl-
360 2 alignment was carried out for 5,000,000 generations with 20 randomly started simultaneous
361 Markov chains (1 cold chain, 19 heated chains) and sampled every 100 generations. ML
362 bootstrap values higher than 50% and Bayesian posterior probabilities are indicated on the
363 Bayesian tree.

364 The outgroup for the metazoan CARD-caspase phylogeny is the only caspase with a
365 CARD pro-domain of the Porifera *Amphimedon queenslandica* (XP_003383519), (Figure 1).
366 Analyses of CARD-caspases were made independently at the deuterostome scale with four
367 different outgroups to test their effect on the stability of the topology: *i*) CARD-caspase-Y of
368 the annelid *Capitella teleta* (ELT97848.1), *ii*) CARD-caspase-2 of the mollusk *Aplysia californica*
369 (XP_005113266), *iii*) CARD-caspase-X2 of cnidarian *Hydra vulgaris* (NP_001274285.1) *iv*)
370 CARD-caspase Ced-3 of the ecdysozoan *Caenorhabditis elegans* (AAG42045.1)
371 (Supplementary Figure 3). For the metazoan Apaf-1 phylogenies, the selected outgroup is
372 Apaf-1 (XP_019855714.1) of Porifera *Amphimedon queenslandica* (Figure S4). For the
373 metazoan Bcl-2 phylogenies, outgroups used to test their effect on stability of the topology
374 are: *i*) Bcl-2-like1 (XP_003383425.1) and Bcl-2-like2 (XP_003387574.1) of Porifera
375 *Amphimedon queenslandica* (Supplementary Figure 5).

376 Topology tests between metazoan CARD-caspase phylogenies from Bayesian inference
377 method and maximum likelihood estimation were evaluated using IQ-TREE[103]. We conducted
378 Kishino-Hasegawa test[104], Shimodaira-Hasegawa test, and approximately unbiased test[105].

379

380 **Estimation of dN/dS**

Codon aligned nucleotide sequences were built using PAL2NAL[106] from clustalo aligned amino acid sequences and gene ORFs. The dN/dS ratio was calculated using EasyCodeML under settings “site model”, nuc-2, and standard icode[61], from the codon aligned nucleotide sequences and newick format trees.

Acknowledgements

Authors particularly acknowledge Helen R Horkan (NUIG, Galway) for help in bioinformatics analysis and helpful comments. Authors thank Sébastien Darras (Sorbonne Université, Banyuls-sur-Mer), Christine Vesque (Sorbonne Université, Paris), Jérôme Gros (Institut Pasteur, Paris), Sabine Hennequin (Sorbonne Université, Paris) and Uri Frank (NUIG, Galway) for helpful comments. GK was supported by a Ph.D. fellowship from the French Ministry of Education, Research and Innovation.

Author Contributions

JP and EQ managed the project. GK made BLAST, phylogenetic and sequences analysis, and figures. GK and EQ wrote the manuscript.

Competing Interest Statement

The authors declare no competing interests.

Data Availability

All data needed to evaluate the conclusions in this study are present in the paper and the Supplementary Materials. Any requests can be addressed to the corresponding author.

BIBLIOGRAPHY

1. Jacobson, M. D., Weil, M. & Raff, M. C. Programmed cell death in animal development. *Cell* **88**, 347–354 (1997).
2. Hipfner, D. R. & Cohen, S. M. Connecting proliferation and apoptosis in development and disease. *Nat Rev Mol Cell Biol* **5**, 805–815 (2004).
3. Vriz, S., Reiter, S. & Galliot, B. Cell death: a program to regenerate. *Curr. Top. Dev. Biol.* **108**, 121–151 (2014).
4. Hengartner, M. O. The biochemistry of apoptosis. *Nature* **407**, 770–776 (2000).
5. Lettre, G. & Hengartner, M. O. Developmental apoptosis in C. elegans: a complex CEDnario. *Nat Rev Mol Cell Biol* **7**, 97–108 (2006).
6. Ellis, H. M. & Horvitz, H. R. Genetic control of programmed cell death in the nematode C. elegans. *Cell* **44**, 817–829 (1986).
7. Bender, C. E. *et al.* Mitochondrial pathway of apoptosis is ancestral in metazoans. *Proc. Natl. Acad. Sci. U.S.A.* **109**, 4904–4909 (2012).
8. Steller, H. Regulation of apoptosis in Drosophila. *Cell Death Differ.* **15**, 1132–1138 (2008).
9. Driscoll, M. Cell death in C. elegans: molecular insights into mechanisms conserved between nematodes and mammals. *Brain Pathol* **6**, 411–425 (1996).
10. Dorstyn, L., Akey, C. W. & Kumar, S. New insights into apoptosome structure and function. *Cell Death Differ* **25**, 1194–1208 (2018).

429 11. Young, N. D. *et al.* Diversity in the intrinsic apoptosis pathway of nematodes. *Commun Biol* **3**, 478
430 (2020).
431 12. Bell, R. A. V. & Megeney, L. A. Evolution of caspase-mediated cell death and differentiation:
432 twins separated at birth. *Cell Death Differ* **24**, 1359–1368 (2017).
433 13. Shrestha, S. *et al.* Caspases from scleractinian coral show unique regulatory features. *J Biol Chem*
434 **295**, 14578–14591 (2020).
435 14. Uren, A. G. *et al.* Identification of Paracaspases and Metacaspases: Two Ancient Families of
436 Caspase-like Proteins, One of which Plays a Key Role in MALT Lymphoma. *Molecular Cell* **6**, 961–
437 967 (2000).
438 15. Crawford, E. D. *et al.* Conservation of caspase substrates across metazoans suggests hierarchical
439 importance of signaling pathways over specific targets and cleavage site motifs in apoptosis. *Cell*
440 *Death Differ* **19**, 2040–2048 (2012).
441 16. Thornberry, N. A. & Lazebnik, Y. Caspases: enemies within. *Science* **281**, 1312–1316 (1998).
442 17. S, E. Apoptosis: a review of programmed cell death. *Toxicologic pathology* vol. 35
443 https://pubmed.ncbi.nlm.nih.gov/17562483/ (2007).
444 18. Galluzzi, L. *et al.* Molecular mechanisms of cell death: recommendations of the Nomenclature
445 Committee on Cell Death 2018. *Cell Death Differ.* **25**, 486–541 (2018).
446 19. Terajima, D. *et al.* Identification of candidate genes encoding the core components of the cell
447 death machinery in the Ciona intestinalis genome. *Cell Death Differ.* **10**, 749–753 (2003).
448 20. Delsuc, F., Brinkmann, H., Chourrout, D. & Philippe, H. Tunicates and not cephalochordates are
449 the closest living relatives of vertebrates. *Nature* **439**, 965–968 (2006).
450 21. Lee, T. V., Kamber Kaya, H. E., Simin, R., Baehrecke, E. H. & Bergmann, A. The initiator caspase
451 Dronc is subject of enhanced autophagy upon proteasome impairment in Drosophila. *Cell Death*
452 *Differ* **23**, 1555–1564 (2016).
453 22. Fogarty, C. E. *et al.* Extracellular Reactive Oxygen Species Drive Apoptosis-Induced Proliferation
454 via Drosophila Macrophages. *Curr Biol* **26**, 575–584 (2016).
455 23. Fan, Y. *et al.* Genetic models of apoptosis-induced proliferation decipher activation of JNK and
456 identify a requirement of EGFR signaling for tissue regenerative responses in Drosophila. *PLoS*
457 *Genet* **10**, e1004131 (2014).

458 24. Fan, Y. & Bergmann, A. The cleaved-Caspase-3 antibody is a marker of Caspase-9-like DRONC
459 activity in Drosophila. *Cell Death Differ* **17**, 534–539 (2010).
460 25. Napoletano, F. *et al.* p53-dependent programmed necrosis controls germ cell homeostasis
461 during spermatogenesis. *PLoS Genet* **13**, e1007024 (2017).
462 26. Lim, Y., Dorstyn, L. & Kumar, S. The p53-caspase-2 axis in the cell cycle and DNA damage
463 response. *Exp Mol Med* **53**, 517–527 (2021).
464 27. Bao, Q. & Shi, Y. Apoptosome: a platform for the activation of initiator caspases. *Cell Death Differ*
465 **14**, 56–65 (2007).
466 28. Jaroszewski, L., Rychlewski, L., Reed, J. C. & Godzik, A. ATP-activated oligomerization as a
467 mechanism for apoptosis regulation: fold and mechanism prediction for CED-4. *Proteins* **39**, 197–
468 203 (2000).
469 29. Zmasek, C. M. & Godzik, A. Evolution of the animal apoptosis network. *Cold Spring Harb Perspect*
470 *Biol* **5**, a008649 (2013).
471 30. Zmasek, C. M., Zhang, Q., Ye, Y. & Godzik, A. Surprising complexity of the ancestral apoptosis
472 network. *Genome Biol.* **8**, R226 (2007).
473 31. Zou, H., Henzel, W. J., Liu, X., Lutschg, A. & Wang, X. Apaf-1, a human protein homologous to C.
474 elegans CED-4, participates in cytochrome c-dependent activation of caspase-3. *Cell* **90**, 405–413
475 (1997).
476 32. Zou, H., Li, Y., Liu, X. & Wang, X. An APAF-1.cytochrome c multimeric complex is a functional
477 apoptosome that activates procaspase-9. *J. Biol. Chem.* **274**, 11549–11556 (1999).
478 33. Dorstyn, L. *et al.* The role of cytochrome c in caspase activation in Drosophila melanogaster cells.
479 *J Cell Biol* **156**, 1089–1098 (2002).
480 34. Shi, Y. Mechanical aspects of apoptosome assembly. *Curr Opin Cell Biol* **18**, 677–684 (2006).
481 35. Li, Y. *et al.* Conservation and divergence of mitochondrial apoptosis pathway in the Pacific oyster,
482 Crassostrea gigas. *Cell Death Dis* **8**, e2915 (2017).
483 36. Kiss, T. Apoptosis and its functional significance in molluscs. *Apoptosis* **15**, 313–321 (2010).
484 37. Romero, A., Novoa, B. & Figueras, A. The complexity of apoptotic cell death in mollusks: An
485 update. *Fish Shellfish Immunol.* **46**, 79–87 (2015).

486 38. Estévez-Calvar, N., Romero, A., Figueras, A. & Novoa, B. Genes of the mitochondrial apoptotic
487 pathway in Mytilus galloprovincialis. *PLoS ONE* **8**, e61502 (2013).
488 39. Srivastava, M. *et al.* The Amphimedon queenslandica genome and the evolution of animal
489 complexity. *Nature* **466**, 720–726 (2010).
490 40. Srivastava, M. *et al.* The Trichoplax genome and the nature of placozoans. *Nature* **454**, 955–960
491 (2008).
492 41. Zermati, Y. *et al.* Nonapoptotic role for Apaf-1 in the DNA damage checkpoint. *Mol Cell* **28**, 624–
493 637 (2007).
494 42. Ferraro, E. *et al.* Apaf1 plays a pro-survival role by regulating centrosome morphology and
495 function. *J Cell Sci* **124**, 3450–3463 (2011).
496 43. Shakeri, R., Kheirollahi, A. & Davoodi, J. Apaf-1: Regulation and function in cell death. *Biochimie*
497 **135**, 111–125 (2017).
498 44. Lee, E. F. *et al.* Discovery and molecular characterization of a Bcl-2-regulated cell death pathway
499 in schistosomes. *Proc. Natl. Acad. Sci. U.S.A.* **108**, 6999–7003 (2011).
500 45. Banjara, S., Suraweera, C. D., Hinds, M. G. & Kvansakul, M. The Bcl-2 Family: Ancient Origins,
501 Conserved Structures, and Divergent Mechanisms. *Biomolecules* **10**, (2020).
502 46. Kalkavan, H. & Green, D. R. MOMP, cell suicide as a BCL-2 family business. *Cell Death Differ* **25**,
503 46–55 (2018).
504 47. Dunn, S. R., Phillips, W. S., Spatafora, J. W., Green, D. R. & Weis, V. M. Highly conserved caspase
505 and Bcl-2 homologues from the sea anemone Aiptasia pallida: lower metazoans as models for
506 the study of apoptosis evolution. *J. Mol. Evol.* **63**, 95–107 (2006).
507 48. Clavier, A., Rincheval-Arnold, A., Colin, J., Mignotte, B. & Guénal, I. Apoptosis in Drosophila:
508 which role for mitochondria? *Apoptosis* **21**, 239–251 (2016).
509 49. Krumschnabel, G., Sohm, B., Bock, F., Manzl, C. & Villunger, A. The enigma of caspase-2: the
510 laymen's view. *Cell Death & Differentiation* **16**, 195–207 (2009).
511 50. Olsson, M., Forsberg, J. & Zhivotovsky, B. Caspase-2: the reinvented enzyme. *Oncogene* **34**,
512 1877–1882 (2015).
513 51. Lassus, P., Opitz-Araya, X. & Lazebnik, Y. Requirement for caspase-2 in stress-induced apoptosis
514 before mitochondrial permeabilization. *Science* **297**, 1352–1354 (2002).

515 52. Zhivotovsky, B. & Orrenius, S. Caspase-2 function in response to DNA damage. *Biochem. Biophys.*
516 *Res. Commun.* **331**, 859–867 (2005).
517 53. Krumschnabel, G., Manzl, C. & Villunger, A. Caspase-2: killer, savior and safeguard--emerging
518 versatile roles for an ill-defined caspase. *Oncogene* **28**, 3093–3096 (2009).
519 54. Olsson, M. *et al.* DISC-mediated activation of caspase-2 in DNA damage-induced apoptosis.
520 *Oncogene* **28**, 1949–1959 (2009).
521 55. Lavrik, I. N., Golks, A., Baumann, S. & Krammer, P. H. Caspase-2 is activated at the CD95 death-
522 inducing signaling complex in the course of CD95-induced apoptosis. *Blood* **108**, 559–565 (2006).
523 56. Braga, M. *et al.* Involvement of oxidative stress and caspase 2-mediated intrinsic pathway
524 signaling in age-related increase in muscle cell apoptosis in mice. *Apoptosis* **13**, 822–832 (2008).
525 57. Duan, H. & Dixit, V. M. RAIDD is a new 'death' adaptor molecule. *Nature* **385**, 86–89 (1997).
526 58. Tinel, A. & Tschopp, J. The PIDDosome, a protein complex implicated in activation of caspase-2 in
527 response to genotoxic stress. *Science* **304**, 843–846 (2004).
528 59. Haupt, S., Berger, M., Goldberg, Z. & Haupt, Y. Apoptosis - the p53 network. *J Cell Sci* **116**, 4077–
529 4085 (2003).
530 60. Eyre-Walker, A. The genomic rate of adaptive evolution. *Trends Ecol Evol* **21**, 569–575 (2006).
531 61. Gao, F. *et al.* EasyCodeML: A visual tool for analysis of selection using CodeML. *Ecol Evol* **9**, 3891–
532 3898 (2019).
533 62. Force, A. *et al.* Preservation of duplicate genes by complementary, degenerative mutations.
534 *Genetics* **151**, 1531–1545 (1999).
535 63. Conant, G. C. & Wolfe, K. H. Turning a hobby into a job: how duplicated genes find new
536 functions. *Nat Rev Genet* **9**, 938–950 (2008).
537 64. Fares, M. A., Keane, O. M., Toft, C., Carretero-Paulet, L. & Jones, G. W. The roles of whole-
538 genome and small-scale duplications in the functional specialization of Saccharomyces cerevisiae
539 genes. *PLoS Genet* **9**, e1003176 (2013).
540 65. Meier, P., Finch, A. & Evan, G. Apoptosis in development. *Nature* **407**, 796–801 (2000).
541 66. Degterev, A., Boyce, M. & Yuan, J. A decade of caspases. *Oncogene* **22**, 8543–8567 (2003).
542 67. Fuchs, Y. & Steller, H. Live to die another way: modes of programmed cell death and the signals
543 emanating from dying cells. *Nat. Rev. Mol. Cell Biol.* **16**, 329–344 (2015).

544 68. Mancini, M. *et al.* Caspase-2 Is Localized at the Golgi Complex and Cleaves Golgin-160 during
545 Apoptosis. *J Cell Biol* **149**, 603–612 (2000).
546 69. Ouyang, Y. *et al.* Dronc caspase exerts a non-apoptotic function to restrain phospho-Numb-
547 induced ectopic neuroblast formation in Drosophila. *Development* **138**, 2185–2196 (2011).
548 70. Huh, J. R., Guo, M. & Hay, B. A. Compensatory proliferation induced by cell death in the
549 Drosophila wing disc requires activity of the apical cell death caspase Dronc in a nonapoptotic
550 role. *Curr. Biol.* **14**, 1262–1266 (2004).
551 71. Kumar, S. & Doumanis, J. The fly caspases. *Cell Death Differ* **7**, 1039–1044 (2000).
552 72. Vogeler, S., Carboni, S., Li, X. & Joyce, A. Phylogenetic analysis of the caspase family in bivalves:
553 implications for programmed cell death, immune response and development. *BMC Genomics* **22**,
554 80 (2021).
555 73. Pirger, Z., Rácz, B. & Kiss, T. Dopamine-induced programmed cell death is associated with
556 cytochrome c release and caspase-3 activation in snail salivary gland cells. *Biol. Cell* **101**, 105–116
557 (2009).
558 74. Romero, A., Estévez-Calvar, N., Dios, S., Figueras, A. & Novoa, B. New insights into the apoptotic
559 process in mollusks: characterization of caspase genes in Mytilus galloprovincialis. *PLoS ONE* **6**,
560 e17003 (2011).
561 75. Zhang, L., Li, L. & Zhang, G. Gene discovery, comparative analysis and expression profile reveal
562 the complexity of the Crassostrea gigas apoptosis system. *Dev. Comp. Immunol.* **35**, 603–610
563 (2011).
564 76. Yang, B. *et al.* Molecular cloning of two molluscan caspases and gene functional analysis during
565 Crassostrea angulata (Fujian oyster) larval metamorphosis. *Mol. Biol. Rep.* **42**, 963–975 (2015).
566 77. Plachetzki, D. C., Pankey, M. S., MacManes, M. D., Lesser, M. P. & Walker, C. W. The Genome of
567 the Softshell Clam Mya arenaria and the Evolution of Apoptosis. *Genome Biol Evol* **12**, 1681–
568 1693 (2020).
569 78. Piquet, B., Shillito, B., Lallier, F. H., Duperron, S. & Andersen, A. C. High rates of apoptosis
570 visualized in the symbiont-bearing gills of deep-sea Bathymodiolus mussels. *PLoS ONE* **14**,
571 e0211499 (2019).

572 79. Sokolova, I. M., Evans, S. & Hughes, F. M. Cadmium-induced apoptosis in oyster hemocytes
573 involves disturbance of cellular energy balance but no mitochondrial permeability transition. *J.*
574 *Exp. Biol.* **207**, 3369–3380 (2004).
575 80. Sokolova, I. M. Apoptosis in molluscan immune defense. *Invertebrate Survival Journal* **6**, 49–58
576 (2009).
577 81. An, H.-K. *et al.* CASP9 (caspase 9) is essential for autophagosome maturation through regulation
578 of mitochondrial homeostasis. *Autophagy* **16**, 1598–1617 (2020).
579 82. Madadi, Z., Akbari-Birgani, S., Monfared, P. D. & Mohammadi, S. The non-apoptotic role of
580 caspase-9 promotes differentiation in leukemic cells. *Biochim Biophys Acta Mol Cell Res* **1866**,
581 118524 (2019).
582 83. Hollville, E. & Deshmukh, M. Physiological functions of non-apoptotic caspase activity in the
583 nervous system. *Semin Cell Dev Biol* **82**, 127–136 (2018).
584 84. Tran, H. T. *et al.* Caspase-9 has a nonapoptotic function in Xenopus embryonic primitive blood
585 formation. *J Cell Sci* **130**, 2371–2381 (2017).
586 85. Tamura, R. *et al.* Starfish Apaf-1 activates effector caspase-3/9 upon apoptosis of aged eggs. *Sci*
587 *Rep* **8**, 1611 (2018).
588 86. Belyi, V. A. *et al.* The origins and evolution of the p53 family of genes. *Cold Spring Harb Perspect*
589 *Biol* **2**, a001198 (2010).
590 87. Lu, W.-J., Amatruda, J. F. & Abrams, J. M. p53 ancestry: gazing through an evolutionary lens. *Nat*
591 *Rev Cancer* **9**, 758–762 (2009).
592 88. Berthelet, J. & Dubrez, L. Regulation of Apoptosis by Inhibitors of Apoptosis (IAPs). *Cells* **2**, 163–
593 187 (2013).
594 89. Ribeiro Lopes, M., Parisot, N., Callaerts, P. & Calevro, F. Genetic Diversity of the Apoptotic
595 Pathway in Insects. in *Evolution, Origin of Life, Concepts and Methods* (ed. Pontarotti, P.) 253–
596 285 (Springer International Publishing, 2019). doi:10.1007/978-3-030-30363-1_13.
597 90. Ribeiro Lopes, M. *et al.* Evolutionary novelty in the apoptotic pathway of aphids. *Proc Natl Acad*
598 *Sci U S A* **117**, 32545–32556 (2020).
599 91. Aubrey, B. J. *et al.* Mutant TRP53 exerts a target gene-selective dominant-negative effect to drive
600 tumor development. *Genes Dev* **32**, 1420–1429 (2018).

601 92. Aubrey, B. J., Kelly, G. L., Janic, A., Herold, M. J. & Strasser, A. How does p53 induce apoptosis
602 and how does this relate to p53-mediated tumour suppression? *Cell Death Differ* **25**, 104–113
603 (2018).
604 93. Gattiker, A., Gasteiger, E. & Bairoch, A. ScanProsite: a reference implementation of a PROSITE
605 scanning tool. *Appl Bioinformatics* **1**, 107–108 (2002).
606 94. Quevillon, E. *et al.* InterProScan: protein domains identifier. *Nucleic Acids Res* **33**, W116-120
607 (2005).
608 95. Katoh, K. & Standley, D. M. MAFFT multiple sequence alignment software version 7:
609 improvements in performance and usability. *Mol. Biol. Evol.* **30**, 772–780 (2013).
610 96. Sievers, F. *et al.* Fast, scalable generation of high-quality protein multiple sequence alignments
611 using Clustal Omega. *Mol. Syst. Biol.* **7**, 539 (2011).
612 97. HALL, T. A. BioEdit : a user-friendly biological sequence alignment editor and analysis program
613 for Windows 95/98/NT. *Nucleic Acids Symp. Ser.* **41**, 95–98 (1999).
614 98. Castresana, J. Selection of conserved blocks from multiple alignments for their use in
615 phylogenetic analysis. *Mol. Biol. Evol.* **17**, 540–552 (2000).
616 99. Guindon, S. *et al.* New algorithms and methods to estimate maximum-likelihood phylogenies:
617 assessing the performance of PhyML 3.0. *Syst. Biol.* **59**, 307–321 (2010).
618 100. Gouy, M., Guindon, S. & Gascuel, O. SeaView version 4: A multiplatform graphical user
619 interface for sequence alignment and phylogenetic tree building. *Mol Biol Evol* **27**, 221–224
620 (2010).
621 101. Tamura, K., Stecher, G. & Kumar, S. MEGA11: Molecular Evolutionary Genetics Analysis
622 Version 11. *Mol Biol Evol* **38**, 3022–3027 (2021).
623 102. Ronquist, F. & Huelsenbeck, J. P. MrBayes 3: Bayesian phylogenetic inference under mixed
624 models. *Bioinformatics* **19**, 1572–1574 (2003).
625 103. Nguyen, L.-T., Schmidt, H. A., von Haeseler, A. & Minh, B. Q. IQ-TREE: A Fast and Effective
626 Stochastic Algorithm for Estimating Maximum-Likelihood Phylogenies. *Mol Biol Evol* **32**, 268–274
627 (2015).

628 104. Kishino, H. & Hasegawa, M. Evaluation of the maximum likelihood estimate of the
629 evolutionary tree topologies from DNA sequence data, and the branching order in hominoidea. *J*
630 *Mol Evol* **29**, 170–179 (1989).
631 105. Shimodaira, H. An approximately unbiased test of phylogenetic tree selection. *Syst Biol* **51**,
632 492–508 (2002).
633 106. Suyama, M., Torrents, D. & Bork, P. PAL2NAL: robust conversion of protein sequence
634 alignments into the corresponding codon alignments. *Nucleic Acids Res* **34**, W609-612 (2006).
635
636
637
638

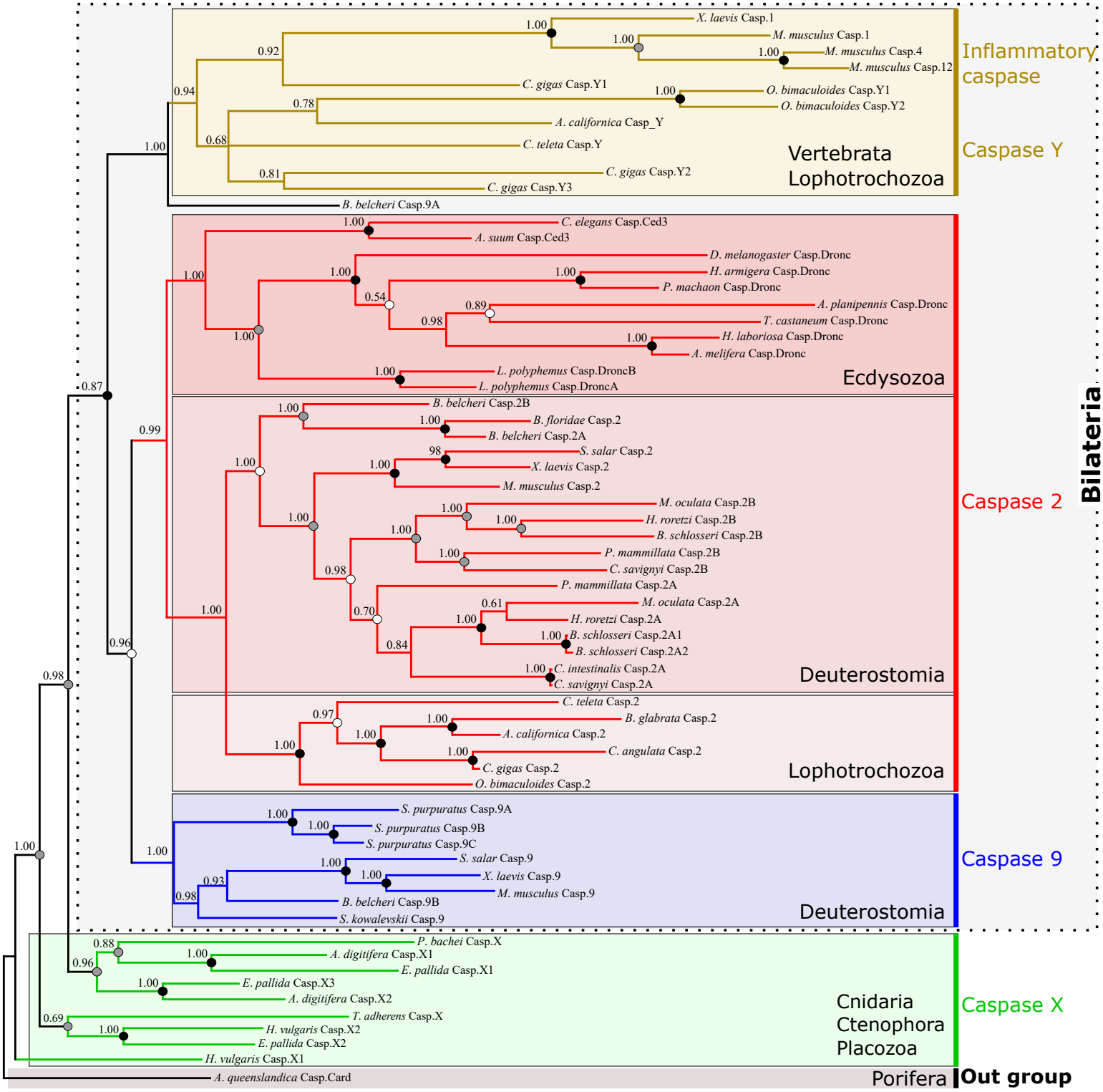

Bayesian posterior probabilities 0 to 1.00

● ML Bootstrap >90

● ML Bootstrap 70-90

○ ML Bootstrap 50-70

Figure 1:

Topology of metazoan CARD-caspase phylogeny obtained by Bayesian inference. Three strongly supported monophyletic groups are identified: caspase-9, caspase-2 and a more heterogeneous group named here [Inflammatory Caspases + Caspase-Y]. Together they form a clade strictly corresponding to bilaterian animals. Caspase-2 is widely distributed among bilaterians [Deutostomia + Ecdysozoa + Lophotrochozoa/Spiralia] reflecting an ancestral origin. Conversely, caspase-9 is strictly restricted to deuterostomian animals. Sequences of non-bilaterians (Cnidaria + Ctenophora + Placozoa) form divergent paraphyletic groups. The selected outgroup is the unique CARD-caspase of Porifera *Amphimedon queenslandica*.

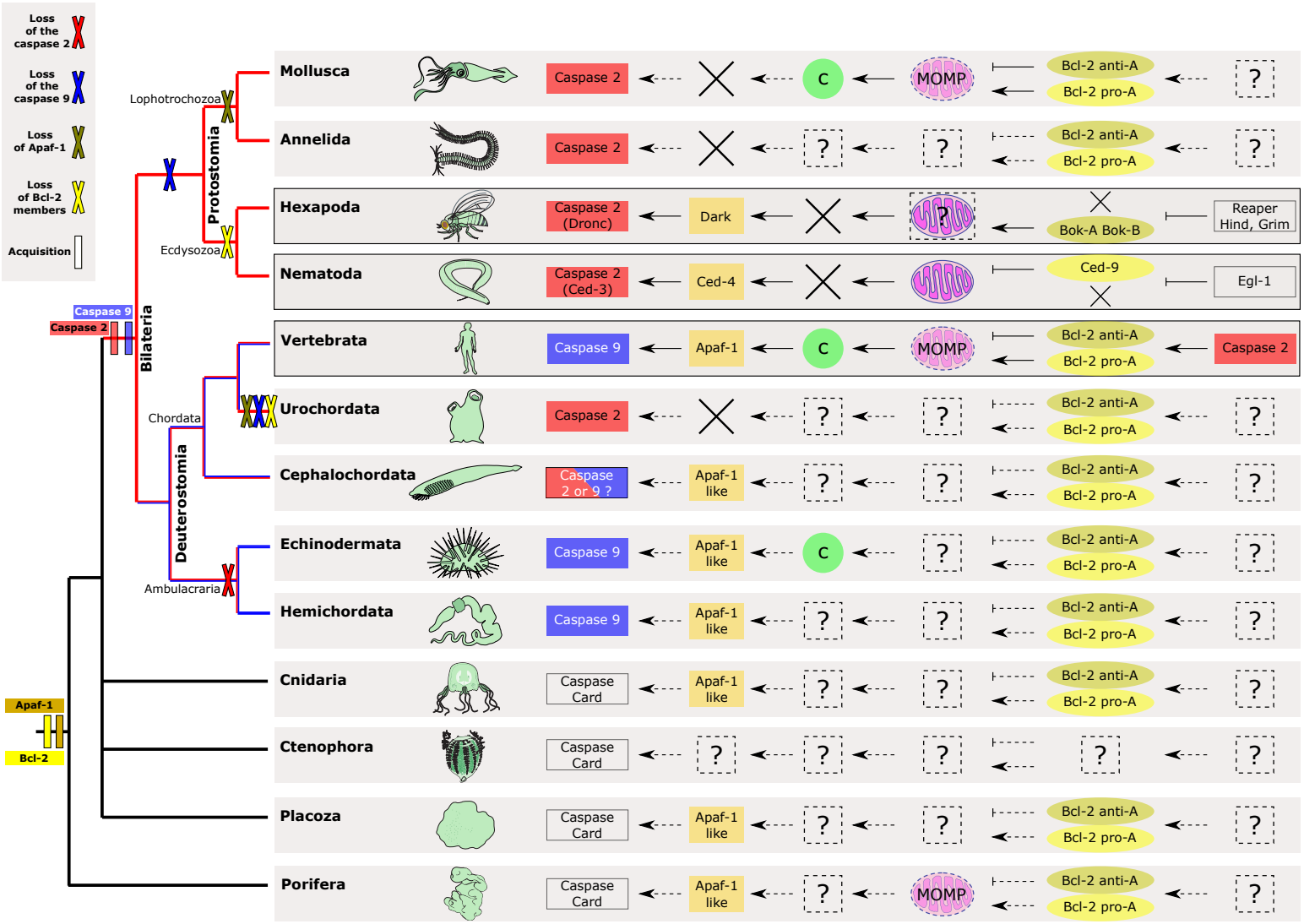
Loss of the caspase 2
Loss of the caspase 9
Loss of Apaf-1
Loss of Bcl-2 members
Acquisition
Caspase 9
Caspase 2
Apaf-1
Bcl-2
Bilateria
Protostomia
Deuterostomia
Lophotrochozoa
Ecdysozoa
Chordata
Ambulacraria
Mollusca
Caspase 2
C
MOMP
Bcl-2 anti-A
Bcl-2 pro-A
?
Annelida
Hexapoda
Caspase 2 (Dronc)
Dark
Bok-A Bok-B
Reaper Hind, Grim
Nematoda
Caspase 2 (Ced-3)
Ced-4
Ced-9
Egl-1
Vertebrata
Caspase 9
Apaf-1
Urochordata
Cephalochordata
Caspase 2 or 9 ?
Apaf-1 like
Echinodermata
Hemichordata
Cnidaria
Caspase Card
Ctenophora
Placoza
Porifera

Figure 2:

Reconstruction of convergent hypothetical intrinsic apoptotic pathways among metazoans according to molecular actors detected and identified in their genomes. Variability of intrinsic apoptotic pathways among animals emerged from convergences and recruitment of distinct actors with independent evolutionary history. Caspase-2 is bilaterian-specific and the initiator of ecdysozoans intrinsic apoptosis. Caspase-9 is restricted to deuterostomes and the specific initiator of mammalian intrinsic apoptosis. Deuterostomes exhibit several losses (i.e. caspase 2 in cephalochordates, caspase 9 in urochordates) or duplication (i.e. caspase 9 in echinoderms), highlighting a putative evolutionary flexibility in apoptotic pathway establishment. Mitochondrial functions diverge among phyla and cytochrome c release thanks to mitochondrial outer membrane permeabilisation (MOMP) is specific only to mammals and possibly echinoderms. The convergent evolutionary histories reflect a probable phylum specific adaptive process leading to parallel evolution of mitochondrial apoptotic pathways observed among animals.

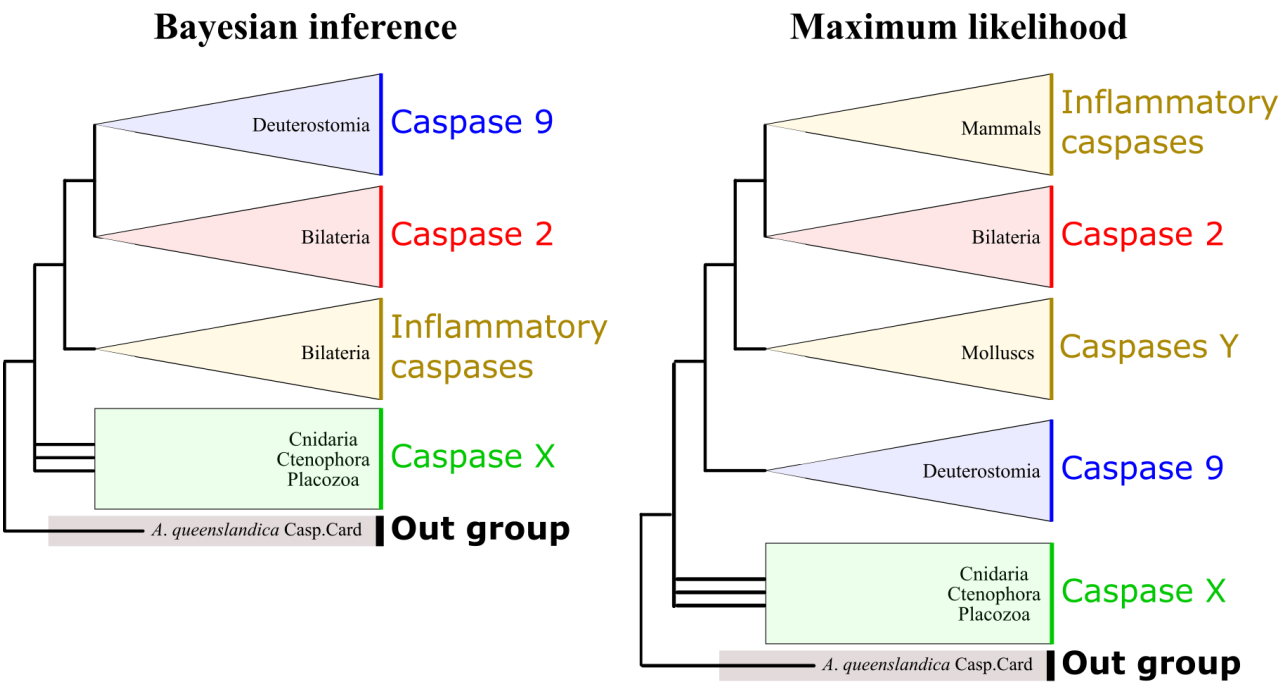

Supplementary Figure 1:

Monophyly of each CARD-caspase group is conserved using Bayesian inference and maximum likelihood analyses. Caspase-9, caspase-2 and [Inflammatory Caspases + Caspase-Y] groups remain conserved, confirming the bilaterian-specificity of caspase-2 and deuterostomian-specificity of caspase-9. Relationships among these three clades differ depending on the methodology employed. Divergent sequences of non-bilaterians animals (Cnidaria + Ctenophora + Placozoa) always form a paraphyletic group of caspases.

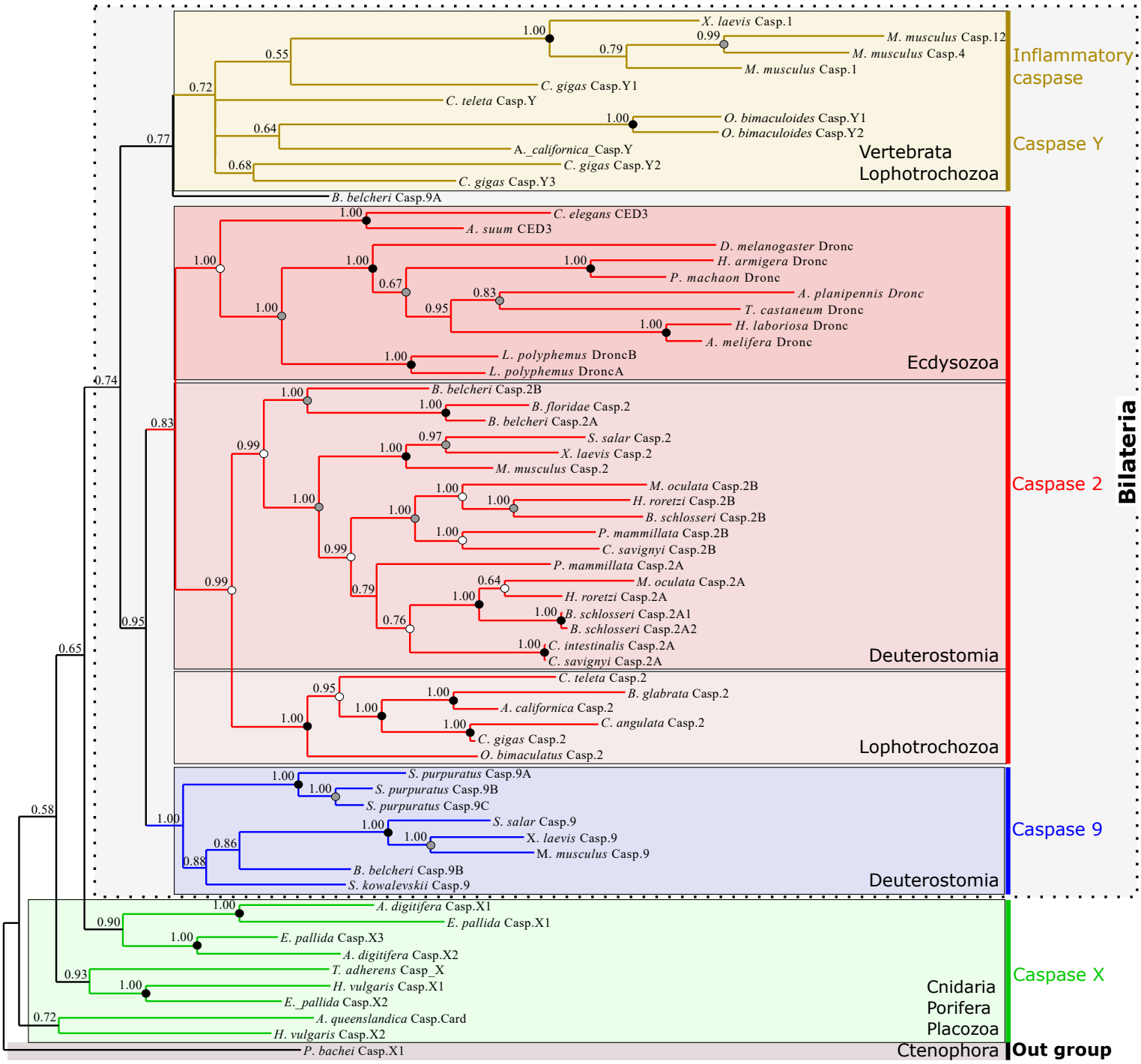

Bayesian posterior probabilities 0 to 1.00

● ML Bootstrap >90

● ML Bootstrap 70-90

○ ML Bootstrap 50-70

Supplementary Figure 2:

Topology of metazoan CARD-caspase phylogeny obtained by Bayesian inference. Selected outgroup is the unique CARD-caspase of Ctenophora *Pleurobrachia bachei.* The three strongly supported monophyletic groups identified, caspase-9, caspase-2 and [Inflammatory Caspases + Caspase-Y], are the same as when we used the unique CARD-caspase of the Porifera *Amphimedon queenslandica* as outgroup. Also, sequences from bilaterian animals remain monophyletic.

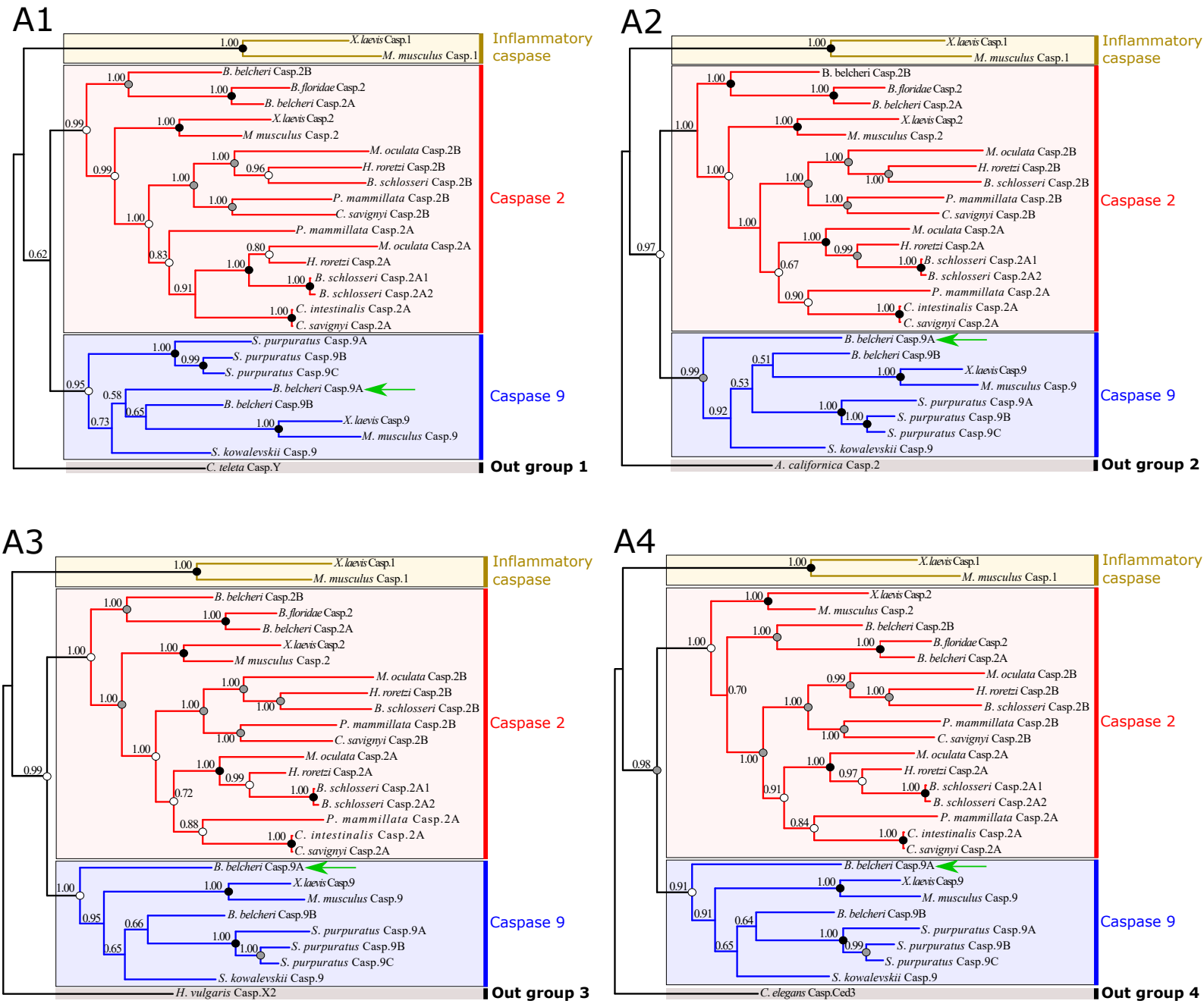

Nodes robustness

Bayesian posterior probabilities 0 to 1.00

● ML Bootstrap >90

● ML Bootstrap 70-90

○ ML Bootstrap 50-70

B.belcheri Casp.9A ←

Supplementary Figure 3:

Phylogeny of CARD-caspases at the deuterostomian scale. Maximum likelihood and Bayesian inference methods produce similar topologies. Despite the unstable position of cephalochordate *Branchiostoma belcheri* caspase-9A (green arrow), it unequivocally appears to belong to the caspase-9 group. Numbers given correspond to posterior probabilities. We used respectively as outgroups *Capitella teleta* caspase-Y (ELT97848.1) (**A1**), *Aplysia californica* caspase-2 (XP_005113266) (**A2**), *Hydra vulgaris* caspase-X2 (NP_001274285.1) (**A3**), and *Caenorhabditis elegans* Ced3 (AAG42045.1) (**A4**).

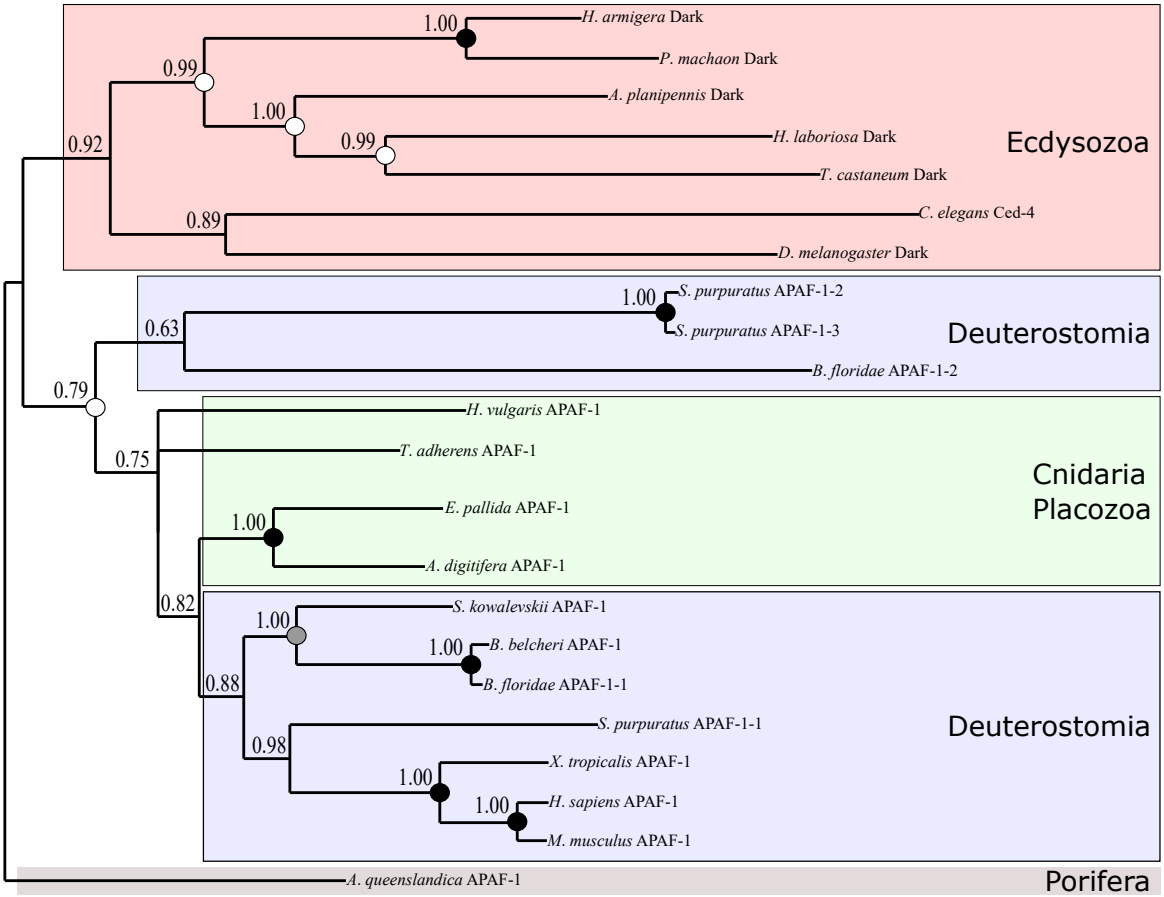

Bayesian posterior probabilities 0 to 1.00

● ML Bootstrap >90

● ML Bootstrap 70-90

○ ML Bootstrap 50-70

Supplementary Figure 4:

Phylogeny of Apaf-1 at the metazoan scale. Two monophyletic groups are identified: Apaf-1 of ecdysozoans, and apaf-1 of [Deutostomia + Cnidaria + Placozoa]. Globally, the topology is not consistent with the species phylogeny, and nodes are poorly supported. Among metazoans, Apaf-1 is characterised by high sequence divergence and fast independent evolution, making homology hypotheses difficult to establish. The selected outgroup is Apaf-1 of Porifera *Amphimedon queenslandica*.

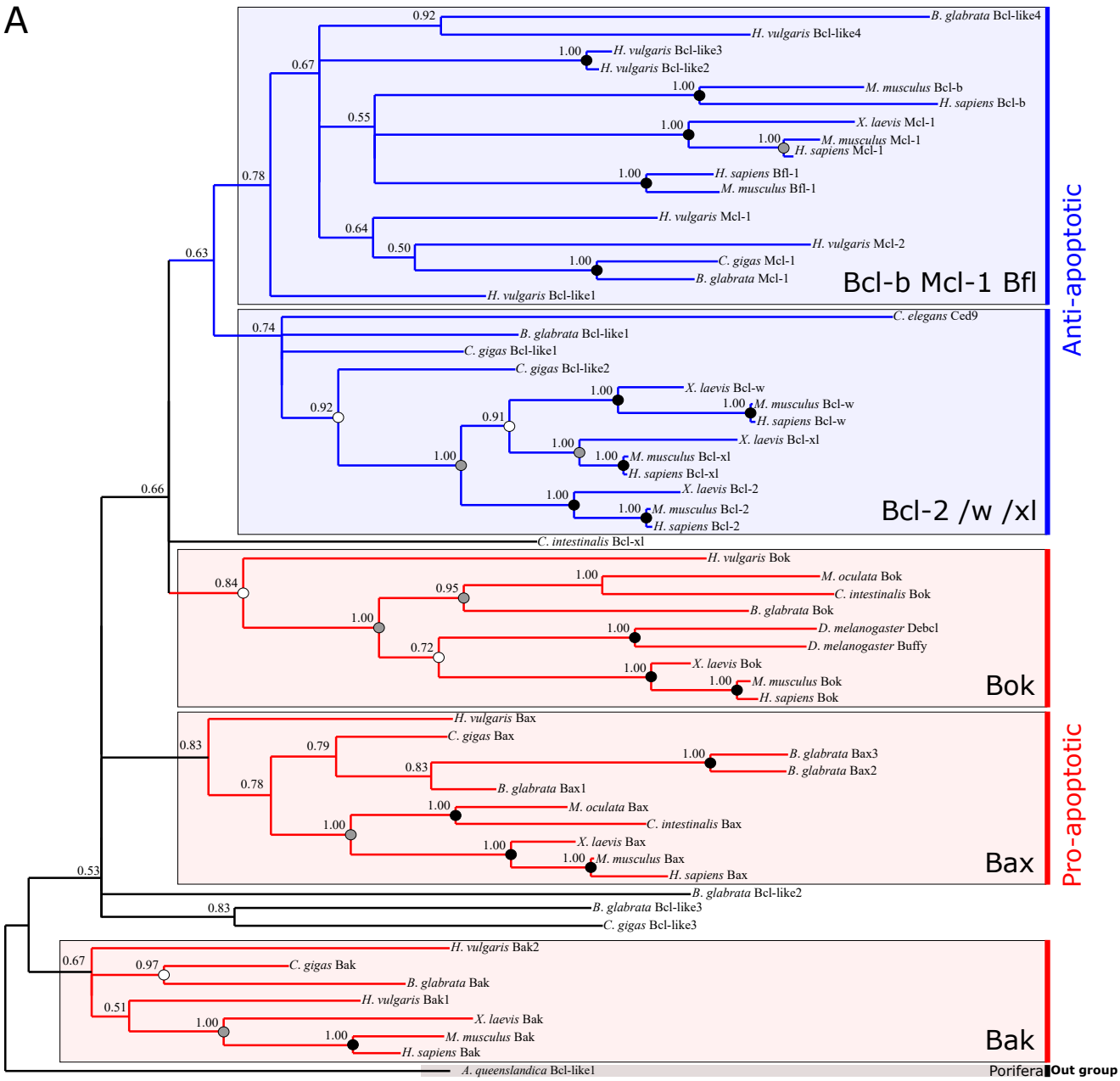

Bayesian posterior probabilities 0 to 1.00

● ML Bootstrap >90

● ML Bootstrap 70-90

○ ML Bootstrap 50-70

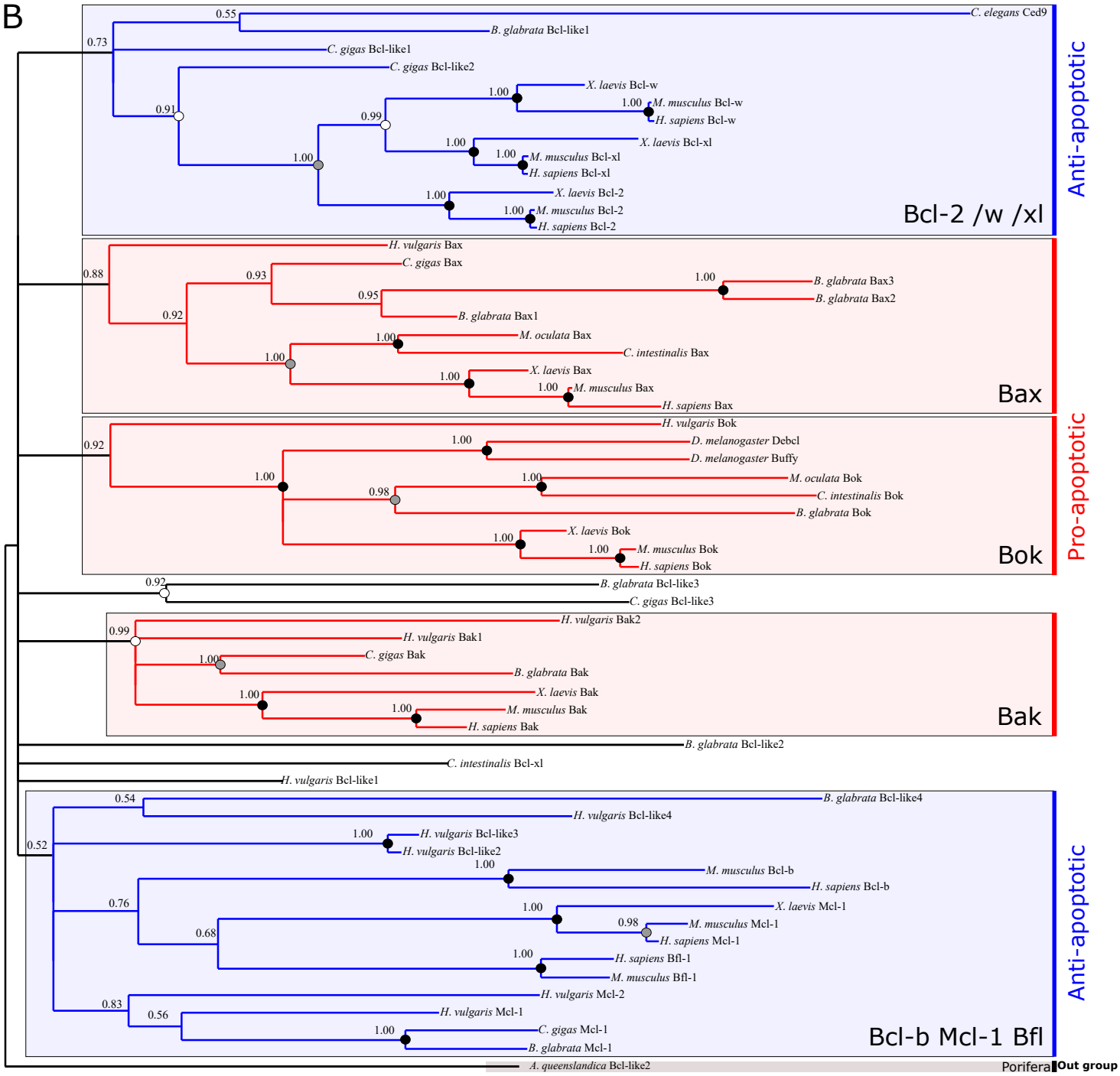

Bayesian posterior probabilities 0 to 1.00

● ML Bootstrap >90

● ML Bootstrap 70-90

○ ML Bootstrap 50-70

Supplementary Figure 5:

Topology of Bcl-2 family phylogeny from Bayesian inference and maximum likelihood at the metazoan scale using outgroups *Amphimedon queenslandica* Bcl-like 1 (XP_003383425.1) (**A**) and Bcl-like 2 (XP_003387574.1) (**B**). Bcl-2 proteins strictly clustered into five monophyletic groups: three 'pro-apoptotic' clades (Bok, Bak, Bax) and two less supported 'anti-apoptotic' groups (Bcl-2/W/XL) and a more complex (Bcl-B/Mcl-1/Bfl-1) clade. Each group includes bilaterian as well as non-bilaterian sequences which suggests a deep origin of this complex multigenic family. Clustering into these five groups is consistent between analyses, while relationships among them is not well resolved.

Supplemental table 1: List of CARD-caspases used for phylogenetic analysis.

Species		Accession number	Name
Porifera	*Amphimedon queenslandica*	XP_003383519.1	Casp. Card
Cnidaria	*Acropora digitifera*	XP_015766400.1	Casp. X2
		XP_015768208.1	Casp. X1
	Exaiptasia pallida	KXJ12672.1	Casp. X1
		KXJ20965.1	Casp. X2
		KXJ12683.1	Casp. X3
	Hydra vulgaris	ACY95435.1	Casp. X1
		ACY95436.1	Casp. X2
Ctenophora	*Pleurobrachia bachei*	Sb 2658116	Casp. X
Placozoa	*Trochoplax adherens*	RDD44781.1	Casp. X
Lophotrocozoa	*Aplysia californica*	XP_005113266.2	Casp. 2
		XP_012945422.1	Casp. Y
	Biomphalaria glabrata	XP_013082356.1	Casp. 2
	Capitella teleta	ELU00616.1	Casp. 2
		ELT97848.1	Casp. Y
	Crassostrea angulata	AGN75137.1	Casp. 2
	Crassostrea gigas	XP_011419292.2	Casp. 2
		XP_011414267.3	Casp. Y1
		XP_011449817.2	Casp. Y3
		XP_011432762.2	Casp. Y2
	Octopus bimaculoides	XP_014783442.1	Casp. 2
		XP_014790087.1	Casp. Y1
		XP_014784582.1	Casp. Y2
Chelicerata	*Limulus polyphemus*	XP_013788138.1	Casp. 2A
		XP_013776997.1	Casp. 2B
Insecta	*Agrilus planipennis*	XP_018324425.1	Casp. 2
	Apis melifera	XP_016771440.1	Casp. 2
	Drosophila melanogaster	CAB53565.1	Casp. 2
	Habropoda laboriosa	XP_017788772.1	Casp. 2
	Helicoverpa armigera	AEK20835.1	Casp. 2
	Papilio machaon	XP_014362236.1	Casp. 2
	Tribolium castaneum	XP_001813274.1	Casp. 2
Nematoda	*Ascaris suum*	ERG86894.1	Casp. 2
	Caenorhabditis elegans	AAG42045.1	Casp. 2
Vertebrata	*Salmo salar*	XP_014009539.1	Casp. 2
		XP_013991583.1	Casp. 9
	Mus musculus	NP_033937.2	Casp. 1
		EDL13489.1	Casp. 2
		NP_031635.2	Casp. 4
		AAH56447.1	Casp. 9
		AAT91067.1	Casp. 12
	Xenopus laevis	NP_001081223.1	Casp. 1
		NP_001081404.1	Casp. 2
		NP_001079035.1	Casp. 9

Echinodermata	*Strongylocentrotus purpuratus*	XP_789183.3	Casp. 9A
		XP_011661242.1 1	Casp. 9B
		XP_011661359.1	Casp. 9C
Hemichordata	*Saccoglossus kowalevskii*	XP_006811879.1	Casp. 9
Cephalochardata	*Branchiostoma belcheri*	XP_019646757.1	Casp. 2A
		XP_019642903.1	Casp. 2B
		XP_019623612.1	Casp. 9A
		XP_019644208.1	Casp. 9B
	Branchiostoma floridae	EEN68002.1	Casp. 2
Urochordata	*Botryllus schlosseri*	Boschl.CG.Botznik2013.chrUn.g02816.01.p	Casp. 2A1
		Boschl.CG.Botznik2013.chrUn.g08767.01.p	Casp. 2A2
		Boschl.CG.Botznik2013.chrUn.g09831.01.p	Casp. 2B
	Ciona intestinalis	KH2012:KH.C4.463.v1.A.ND1-1	Casp. 2A
	Ciona savignyi	CISAVI-CG-ENS81-R15-461426-463207-09349-P	Casp. 2A
		CISAVI-CG-ENS81-R54-461275-467018-10343-P	Casp. 2B
	Molgula oculata	Moocul-CG-ELv1_2-S113854-g13164-01-p	Casp. 2A
		Moocul-CG-ELv1_2-S103067-g09526-01-p	Casp. 2B
	Phallusia mammillata	PHMAMM-CG-MTP2014-S310-G07060-01-P	Casp. 2A
		PHMAMM-CG-MTP2014-S92-G02989-01-P	Casp. 2B
	Halocynthia roretzi	HARORE-CG-MTP2014-S35-G03390-01-P	Casp. 2A
		HARORE-CG-MTP2014-S130-G07320-01-P	Casp. 2B

Supplemental Table 2: Topology tests between Bayesian inference method (BI topology) and maximum likelihood estimation (ML topology). p-KH : p-value of one sided Kishino-Hasegawa test. p-SH : p-value of Shimodaira-Hasegawa test. p-AU : p-value of approximately unbiased (AU) test. In all cases, BI topology is more likelihood than the ML topology.

	p-KH	p-SH	p-AU
BI topology	0.714	1	0.702
ML topology	0.286	0.286	0.298

Supplemental Table 3: List of Apaf-1 among metazoans. N/A: No APAF-1 has been identified.

Species		Accession number
Porifera	*Amphimedon queenslandica*	XP_019855714.1
Ctenophora	*Pleurobrachia bachei*	N/A
Placozoa	*Trichoplax sp.*	RDD40813.1
Cnidaria	*Acropora digitifera*	XP_015776356.1
	Exaiptasia pallida	KXJ17575.1
	Hydra vulgaris	CDG72123.1
Nematoda	*Caenorhabditis elegans*	CAA48781.1
Insecta	*Agrilus planipennis*	XP_025834330.1
	Drosophila melanogaster	NP_725637.1
	Habropoda laboriosa	XP_017794472.1
	Helicoverpa armigera	XP_021181657.1
	Papilio machaon	XP_014359375.1
	Tribolium castaneum	XP_015840766.1
	Aplysia californica	N/A
	Biomphalaria glabrata	N/A
Lophotrocozoa	*Crassostrea angulata*	N/A
	Crassostrea gigas	N/A
	Octopus bimaculoides	N/A
	Capitella teleta	N/A
Vertebrata	*Homo sapiens*	XP_047284715.1
	Mus musculus	NP_033814.2
	Xenopus laevis	NP_001085834.1
Echinodermata	*Strongylocentrotus purpuratus*	XP_011682983.1 XP_011680781.1 XP_011680779.1
Hemichordata	*Saccoglossus kowalevskii*	XP_006818297.1
Cephalochordata	*Branchiostoma belcheri*	XP_019621685.1
	Branchiostoma floridae	XP_035681983.1 XP_035678916.1
Urochordata	*Botryllus schlosseri*	N/A
	Ciona intestinalis	N/A

	Ciona savignyi	N/A
	Molgula oculata	N/A
	Phallusia mammillata	N/A
	Halocynthia roretzi	N/A

Supplemental table 4: List of Bcl-2 used for phylogenetic analysis.

Species		Accession number	Names
Porifera	*Amphimedon queenslandica*	XP_003383425.1	Bcl-2 like 1
		XP_003387574.1	Bcl-2 like 2
Cnidaria	*Hydra vulgaris*	EF104645.1	Bak 1
		EU035760.1	Bak 2
		XP_012562061.1	Bax
		EU035764.1	Bcl-2 like 1
		EF104646.1	Bcl-2 like 2
		EU035765.1	Bcl-2 like 3
		EU035763.1	Bcl-2 like 4
		EU035761.1	Bok
		EF104647.1	Mcl-1 1
		EU035762	Mcl-1 2
Nematoda	*Caenorhabditis elegans*	AAA20080.1	Ced-9
Insecta	*Drosophila melanogaster*	AAF44120.1	Buffy (Bok-1)
		AAF26289.1	Buffy (Bok-2)
Lophotrocozoa	*Biomphalaria glabrata*	XP_013085524.1	Bax 1
		XP_013096338_1	Bax 2
		XP_013086802.1	Bax 3
		XP_013070177.1	Bak
		XP_013081872.1	Bcl-2 like 1
		XP_013093137.1	Bcl-2 like 2
		XP_013068612.1	Bcl-2 like 3
		XP_013083436.1	Bcl-2 like 4
		XP_013069706.1	Bok
		XP_013065969.1	Mcl-1
	Crassostrea gigas	XP_011424481.1	Bax
		XP_011439700.1	Bak
		XP_011449013.1	Bcl-2 like 1
		ACH42081.1	Bcl-2 like 2
		EKC18663.1	Bcl-2 like 3
		XP_011436990.1	Mcl-1 1
		EKC40007.1	Mcl-1 2
Vertebrata	*Homo sapiens*	AAA74466.1	Bak

		NP_001278357.1	Bax
		API71171.1	Bcl-2
		AAK48715.1	Bcl-B
		AAB09055.1	Bcl-w
		CAA80661.1	Bcl-xL
		NP_004040.1	Bfl-1
		NP_115904.1	Bok
		AAF64255.1	Mcl-1
	Mus musculus	NP_031549.2	Bak
		NP_031553.1	Bax
		AAH95964.1	Bcl-2
		Q9Z0F3.1	Bcl-B
		AAA51039.1	Bcl-xL
		AAB09056.1	Bcl-w
		Q07440.1	Bfl-1
		NP_058058.1	Bok
		NP_032588.1	Mcl-1
	Xenopus laevis	NP_001089587.1	Bak
		AAR84081.1	Bax
		BAH28834.1	Bcl-2
		AAI10791.1	Bcl-xl
		XP_018089640.1	Bcl-w
		NP_001139563.1	Bok
		ACI47310.1	Mcl-1
Urochordata	*Ciona intestinalis*	KH2012:KH.C4.794.v1.A.SL1-1	Bax
		KH2012:KH.S653.2.v2.A.SL1-1	Bcl-xl
		KH2012:KH.L87.39.v1.A.ND1-1	Bok
	Molgula oculata	Moocul.CG.ELv1_2.S96550.g08147.01.p	Bax
		Moocul.CG.ELv1_2.S112899.g12639.01.p	Bok